LETTER Communicated by Klaus Hepp

Analog VLSI-Based Modeling of the Primate Oculomotor System

Timothy K. Horiuchi
Christof Koch
Computation and Neural Systems Program, California Institute of Technology, Pasadena, CA 91125, U.S.A.

One way to understand a neurobiological system is by building a simulacrum that replicates its behavior in real time using similar constraints. Analog very large-scale integrated (VLSI) electronic circuit technology provides such an enabling technology. We here describe a neuromorphic system that is part of a long-term effort to understand the primate oculomotor system. It requires both fast sensory processing and fast motor control to interact with the world. A one-dimensional hardware model of the primate eye has been built that simulates the physical dynamics of the biological system. It is driven by two different analog VLSI chips, one mimicking cortical visual processing for target selection and tracking and another modeling brain stem circuits that drive the eye muscles. Our oculomotor plant demonstrates both smooth pursuit movements, driven by a retinal velocity error signal, and saccadic eye movements, controlled by retinal position error, and can reproduce several behavioral, stimulation, lesion, and adaptation experiments performed on primates.

1 Introduction

Using traditional software methods to model complex sensorimotor interactions is often difficult because most neural systems are composed of very large numbers of interconnected elements with nonlinear characteristics and time constants that range over many orders of magnitude. Their mathematical behavior can rarely be solved analytically, and simulations slow dramatically as the number of elements and their interconnections increase, especially when capturing the details of fast dynamics is important. In addition, the interaction of neural systems with the physical world often requires simulating both the motor system in question and its environment, which can be more difficult or time-consuming than simulating the model itself.

Mead (1989b, 1990) and others (Koch, 1989; Douglas, Mahowald, & Mead, 1995) have argued persuasively that an alternative to numerical simulations on digital processors is the fabrication of electronic analogs of neurobiological systems. While parallel, analog computers have been used before to simulate retinal processing and other neural circuits (e.g., Fukushima,

Yamaguchi, Yasuda, & Nagata, 1970), the rapid growth of the field of synthetic neurobiology—the attempt to understand neurobiology by building functional models—has been made possible by using commercial chip fabrication processes, which allow the integration of many hundred thousand transistors on a square centimeter of silicon. Designing massively parallel sensory processing arrays on single chips is now practical. Much has happened in this field in the past eight or so years, producing a considerable number of new analog complementary metal oxide semiconductor (CMOS) building blocks for implementing neural models. Local memory modification and storage (Hasler, Diorio, Minch, & Mead, 1995; Diorio, Hasler, Minch, & Mead, 1997), redundant signal representations, and, most recently, long-distance spike-based signaling (Mahowald, 1992; Boahen, 1997; Mortara, 1997; Kalayjian & Andreou, 1997; Elias, 1993) now form part of the designer's repertoire.

In this article, we review work in our laboratory using neuromorphic analog VLSI techniques to build an interactive, one-dimensional model of the primate oculomotor system. The system consists of two chips: a visual attention-based, tracking chip and an oculomotor control chip. With the continued growth of this system, we hope to explore the system-level consequences of design using neurobiological principles.

1.1 Analog VLSI Approaches for Neural Modeling. The two main arguments for modeling biological systems in analog VLSI are its high speed of information processing and the potential benefits of working within similar design constraints.

The human brain contains on the order of 10^{11} neurons. Although no digital simulation that we know of attempts to simulate the brain of an entire organism (including any species of Nematode),[1] eventually such simulations will be desirable. Nearly all neural models are composed of fine-grained parallel-processing arrays, and implementing such models on serial machines usually results in low simulation speeds orders of magnitude away from real time. The investigation of sensorimotor systems is one example situation where the interaction with the real world must either be adequately simulated inside the computer or the simulation must run quickly enough to interface with a physical model. Typically, a sufficiently realistic simulation of the real world is impractical. Spike-based circuit modeling is another example where simulations can be particularly slow since large, fast swings in voltage are frequent. Additionally, mixing widely disparate time scales within the same simulation leads to stiff differential equations, which are notoriously slow to solve (e.g., learning in spiking networks). Provided the analog VLSI circuitry can produce the proper level of detail and is configurable for the types of models under investigation, neuromorphic

[1] The most detailed simulation of *C. elegans*, which has only 302 neurons, involves but 10% of the neurons (Niebur & Erdös, 1993).

analog VLSI models deliver the speed desirable for large-scale, real-time simulations. Furthermore, augmenting the system to accommodate more neurobiological detail or expanding the size of the sensory array does not affect the speed of operation.

A second intriguing, yet more controversial, argument for the use of VLSI analogs to understand the brain revolves around the claim that certain constraints faced by the analog circuit designer are similar to the constraints faced by nervous systems during evolution and development.

When designing analog circuits to operate in the natural world, the circuit designer must operate within a set of powerful constraints: (1) power consumption, when considering mobile systems, is important; (2) the sensory input array must deal with physical signals whose amplitude can vary up to 10 orders of magnitude; (3) component mismatch and noise limit the precision with which individual circuit components process and represent information; (4) since conventional VLSI circuits are essentially restricted to the surface of the silicon chip, there is a large cost associated with dense interconnection of processing units on a single chip.

All of these constraints also operate in nervous systems. For instance, the human brain, using 12 to 15 W of power,[2] must have evolved under similar pressure to keep the total power consumed to a minimum (Laughlin, van Steveninck, & Anderson, 1998; Sarpeshkar, 1997). Neurons must also solve the problems of mismatch, noise, and dynamic range. The wiring problem for the brain is severe and constrains wiring to relatively sparse interconnection. Although the general computing paradigm at the heart of the digital computer implies that in principle all of these constraints could be implemented in software simulations, in practice they rarely are. The reasons for this are convenience and simulation speed.

There are, of course, limitations of analog VLSI design that are not found in the biological substrate (such as the two-dimensional substrate, or the lack of a technology that would allow wires to grow and to extend connections similar to filopodia) and some constraints in the biological substrate that are not found in analog VLSI (such as low-resistance wiring, viability throughout development, and evolutionary back-compatibility). By understanding the similarities and differences between biology and silicon technology and by using them carefully, it is possible to maintain the relevance of these circuits for biological modeling and gain insight into the solutions found by evolution.

1.2 Biological Eye Movements. Primate eye movements represent an excellent set of sensorimotor behaviors to study with analog VLSI for several reasons. From the motor control perspective, the oculomotor system has a relatively simple musculature, and there is extensive knowledge of

[2] The same power budget as the Mars Sojourner!

the neural substrate driving it. Behaviorally, the primate eye shows a diversity of movements involving saccades (quick, reorienting movements), the vestibulo-ocular reflex (an image-stabilizing movement driven by the head velocity–sensitive semicircular canals), the optokinetic reflex (an image-stabilizing movement driven by wide-field image motion), smooth pursuit (a smooth movement for stabilizing subregions of an image), and vergence (binocular movements to foveate a target with both eyes). The required complexity of visual processing ranges from coarse temporal-change detection (for triggering reflexive saccades) to accurate motion extraction from subregions of the visual field (for driving smooth pursuit) to much more sophisticated processes involving memory, attention, and perception. Perhaps the most attractive aspect of eye movements is that the input and output representations have been well explored, and the purpose of eye movements is fairly clear.

Although the human eye has a field of view of about 170 degrees, we see best in the central 1 degree, or fovea, where the density of photoreceptors is the greatest. Our eyes are constantly moving to scrutinize objects in the world with the fovea. Since visual acuity rapidly declines if retinal slip exceeds 2 or 3 degrees (Westheimer & McKee, 1975), our smooth eye movements are concerned with stabilizing these images.

While the optokinetic reflex (OKR) uses whole-field visual motion to drive image-stabilizing eye movements, smooth pursuit eye movements are characterized by their use of subregions of the field of view. Smooth pursuit allows primates to track small objects accurately even across patterned backgrounds. Interestingly, smooth pursuit eye movements are found only in primates.

While the eye movements described above are concerned with image stabilization, much of our visual behavior involves scanning a scene, moving from one part of an image to another. Saccadic eye movements are employed for this purpose, moving the eyes very rapidly to place visual objects onto the fovea. Saccades are rapid, reaching peak velocities of 600 degrees per second in humans, and last between 25 and 200 msec dependent on the saccade amplitude. Although saccades are fast, they have a relatively long latency, requiring between 150 msec and 250 msec from the onset of a visual target to the beginning of the observed movement (Becker, 1989). These are the only conjugate eye movements that humans can generate as voluntary acts (Becker, 1989). We are able to trigger saccades to visual, auditory, memorized, or even imagined targets.

2 A One-Dimensional Oculomotor Plant

In this section we describe the construction and performance of our one-dimensional oculomotor plant and the architecture of the analog VLSI chip, which controls the motors for both saccadic and smooth pursuit eye movements.

2.1 The Physical Plant. The primate eye is driven by three sets of muscles: the horizontal, vertical, and oblique muscles. These muscles and other suspensory tissues hold the eye in its socket, producing mechanical dynamics with which the control circuits in the brain stem must contend. Both the muscles and the suspensory tissues are elastic and, in the absence of motorneuron activation, will return the orb to a forward-facing position. Both also provide significant viscosity, producing an over-damped, spring–mass system.

While many different models of the oculomotor plant have been proposed to describe the physical dynamics (e.g., Westheimer, 1954; Robinson, 1964), a linear, second-order model of the form:

$$\frac{\theta(s)}{T_{ext}(s)} = \frac{1}{(1 + s\alpha_1)(1 + s\alpha_2)} \tag{2.1}$$

$$\alpha_1, \alpha_2 = \frac{m}{2I} \pm \frac{1}{2I}\sqrt{m^2 - 4kI}\,, \tag{2.2}$$

has been the most widely used. In equation 2.2, k is the spring-constant, m is the damping coefficient, I is the rotational inertia, $\theta(s)$ represents the gaze angle, and $T_{ext}(s)$ represents the externally applied torque. The measured dominant time constant in the eye has been found to be approximately 250 msec (Robinson, 1964; Keller, 1973). The force-length relationship of the eye muscles was first measured by Collins, O'Meara, and Scott (1975) by recording the agonist muscle tension required to hold the eye at different eye positions. While this relationship was fit well with a parabolic function, the combination of forces from both muscles tends to cancel the nonlinearity, producing a more-or-less linear force position relationship.

The oculomotor plant model we have constructed is a 1 degree-of-freedom turntable (see Figure 1) driven by a pair of antagonistically pulling DC (direct current) motors. The DC motors are used to generate torque on the eye by creating tension on the ends of a thread attached at its center to the front of the turntable. The viscoelastic properties of the oculomotor plant are simulated electronically by measuring the angle and angular velocity of the eye and driving the motors to generate the appropriate torques on the eye. This allows the demonstration of the viscoelastic mechanical properties by directly manipulating the mechanical system. Because the biological dynamics are not too far from linear (Collins et al., 1975), the system's dynamics have been modeled as linear to simplify analysis and construction.

In the biological system, the fixation position is determined by the balance point of the agonist muscle tension and the passive elastic forces of all the muscle and suspensory tissues. In the hardware model, however, the two motors are not driven directly against each other (with one motor simulating the active muscle and the other motor simulating the combined elastic forces); rather, the calculated difference in forces is applied to only

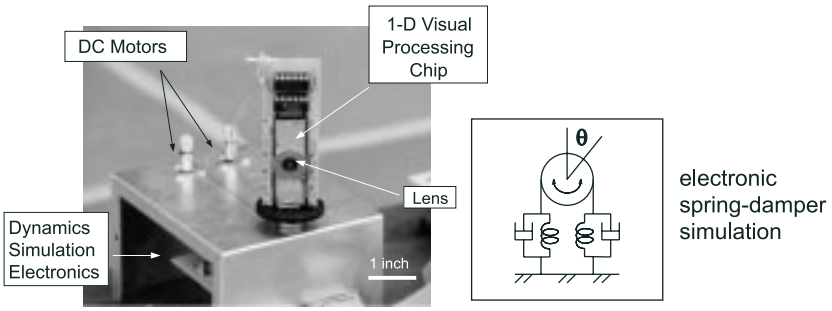

Figure 1: The one-dimensional oculomotor plant. Two DC motors pull on both ends of a drive thread wrapped around the circumference of a small turntable. An analog silicon retina (described in section 3) is mounted vertically on the turntable for reduced rotational inertia. A lens is mounted directly onto the face of the chip to focus an image onto the silicon die. An electronic circuit (mounted inside the box) simulates the mechanical dynamics of the primate oculomotor plant, implementing an overdamped spring-mass system.

one motor. This type of differential drive avoids the increased motor-bearing friction resulting from driving the two motors directly against each other. In addition to the primary motor signals, a small, tonic drive on both motors prevents slack in the thread from building up.

2.2 The Saccadic Burst Generator and Neural Integrator. To drive the oculomotor plant described in the previous section, the brain stem control circuitry must provide the proper signals to overcome both tissue elasticity and viscosity. In order to maintain fixation away from the center position, a sustained pulling force must be generated. Also, to complete an eye movement faster than the eye's natural time constant, a large, transient, acceleration force must be generated (Robinson, 1973). Both the transient and sustained component signals can be found in brain stem areas that drive the motor-neuron pools (Strassman, Highstein, & McCrea, 1986; Godaux & Cheron, 1996). Accurate balancing of these two component signals is necessary and is observed in the motor-neurons driving the eye muscles. If the transient component is too large, the eye will overshoot the target position, and the eye will drift backward to equilibrium; if the transient is too small, the eye undershoots the target, and the eye drifts onward to equilibrium after the saccade.

To generate these oculomotor control signals, we have designed an analog VLSI circuit (see Figure 2), based on models by Jürgens, Becker, & Ko-

rnhuber (1981), McKenzie and Lisberger (1986), and Nichols and Sparks (1995), consisting of three main parts: the saccadic burst generator (which converts desired eye displacement to a velocity signal), the neural integrator (which integrates velocity signals to position signals), and the smooth pursuit integrator (which integrates acceleration signals to velocity signals). For saccadic eye movements, only the first two are used. The saccadic burst integrator is used to control the burst duration, and the neural integrator holds a dynamic memory of the current eye position. This model uses initial motor error (the difference in position from the current gaze angle and the desired gaze angle) as the input to the system. Motor error represents the desired saccade vector that is easily derived from the retinal position of target, relative to the fovea.

Figure 2 shows the block diagram of the oculomotor control circuitry. The input signal to the burst generator is a voltage, V_{in}, specifying the amplitude and direction of the saccade. This signal is held constant for the duration of the saccade. The model generates two signals: a transient pulse of spiking activity (see Figure 3A, signal A) and a step (signal B) of spiking activity, are combined as input to the motor units (signal C). A pair of these transient-step signals drives the two motors of the eye.

Saccades are coordinated in this model by a pause system (not shown), which inhibits the burst generator until a trigger stimulus is provided. The trigger stimulus also activates a sample-and-hold circuit, which holds V_{in} constant throughout the saccade. During a saccade, the input, V_{in}, is continuously compared to the output of the burst integrator, which integrates the burst unit's spike train. The burst neuron keeps emitting spikes until the difference is zero. This arrangement has the effect of firing a number of spikes proportional to the initial value of motor error, consistent with the behavior of short-lead burst neurons found in the saccade-related areas of the brain stem (Hepp, Henn, Vilis, & Cohen, 1989). In the circuit, the burst integrator is implemented by electrical charge accumulating on a 1.9 pF capacitor. After the burst is over, the burst (or eye displacement) integrator is reset to zero by the "pause" circuitry. This burst of spikes serves to drive the eye rapidly against the viscosity.

The burst of activity is also integrated by the neural integrator (converting velocity commands to changes in eye position), which holds the local estimate of the current eye position from which the tonic signal is generated. The neural integrator provides two output spike trains that drive the left and right sustained components of the motor command. The motor units receive inputs from both the saccadic burst units and the neural integrator and compute the sum of these two signals. Figure 3A, signal C shows output data from the burst generator chip, which is qualitatively similar to spike trains seen in the motor neurons of the abducens nucleus of the rhesus monkey (see Figure 3B; King, Lisberger, & Fuchs, 1986).

In addition to the saccadic burst generation circuitry, external inputs have been included to allow the smooth pursuit system to drive the eye

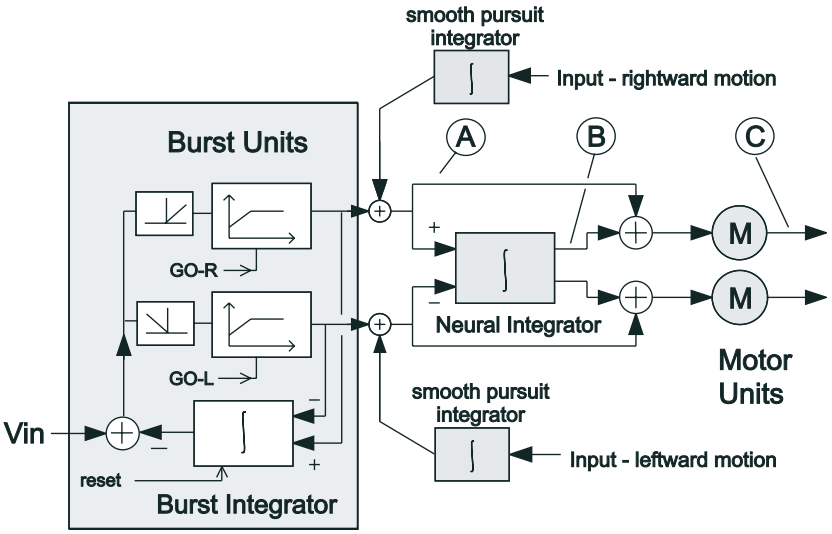

Figure 2: Block diagram of the oculomotor control circuitry. Saccadic eye movements are driven by the burst units to a given displacement determined by the input, V_{in}, provided by the retinal location of the visual target. Smooth pursuit eye movements are driven by the pursuit integrators, which output eye velocity commands. The pursuit integrators receive a target's retinal slip as their input and provide an eye velocity signal as their output. Eye velocity signals are then integrated to eye position (neural integrator), thereby maintaining a memory of the current eye position. The motor unit outputs are an appropriately weighted combination of the velocity and position signals, given the dynamics of the oculomotor plant. Signals A, B, and C for a saccadic eye movement are shown in Figure 3A. See the text for an explanation of the burst units.

motors through the common motor output pathway. This input and its use in smooth pursuit will be discussed in section 3.3.

2.3 Performance. By connecting the motor outputs to the oculomotor plant, saccadic eye movements can be generated. For testing purposes, all of the saccadic eye movements in this section were specified by an external signal. In section 3, saccades were guided by stimuli presented to a one-dimension visual tracking chip mounted on the eye.

Figure 3A shows an example of a saccade with its underlying control signals, and Figure 4A shows an overlay of 20 saccadic trajectories. Figure 4B shows the peak velocity of these 20 saccades as a function of the commanded saccade amplitude. Similar to the peak velocity versus amplitude relation-

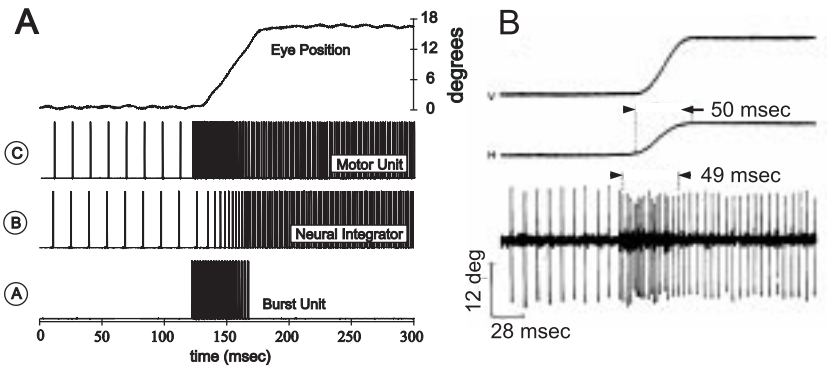

Figure 3: (A) The eye position, burst unit, neural integrator output, and motor unit spike trains during a small saccade. The initial horizontal eye position is off-center, with the neural integrator providing the tonic holding activity. All three spike trains are digital outputs (0 to 5 volts). Only the motor unit output (C) is used externally. The small oscillation seen in the eye position trace is due to the pulse-frequency modulation technique used to drive the eye. Eye position is measured directly using the potentiometer, which doubles as the mechanical bearing for the system. (B) Motor neuron spike train with horizontal (H) and vertical (V) eye position shown during an oblique saccade in a rhesus monkey. (From King et al., 1986)

ship in primate saccades, the peak velocity increases for increasing saccade amplitude and then saturates. As the peak velocity of the saccades saturates, the duration of the saccades begins to increase linearly with amplitude. This saturation is due to the saturating transfer function in the burst unit. These characteristics are qualitatively consistent with primate saccades (Becker, 1989).

2.4 Adaptation of Postsaccadic Drift. Through repeated experience in the world, nearly all animals modify their behavior on the basis of some type of memory. The ability to adapt and learn is not simply an added feature of neural systems; it is a fundamental mechanism that drives the development of the brain and may explain much about the structures and representations that it uses to compute. For this reason, we are beginning to explore the use of adaptation in our oculomotor system. Although there are many different forms of adaptation and learning in the saccadic system, we focus on a particular form that has been implemented in our system.

In the generation of saccades, the sustained (or tonic) component of the command determines the final eye position, while the ideal transient (or

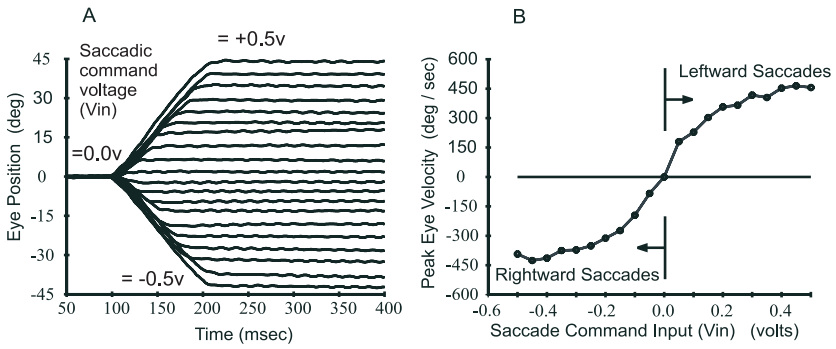

Figure 4: (A) Angular eye position versus time for 20 traces of different saccades triggered from the center position. The input was swept uniformly for different saccade amplitudes from leftward to rightward. The small oscillations in the eye position are due to the discrete pulses used to drive the eye motors; at rest, the pulses are at their lowest frequency and thus most visible. (B) Plot of the peak velocity during each of the saccades on the left. These velocities were computed by performing a least-squares fit to the slope of the center region of the saccade trace. Peak velocities of up to 870 degrees per second have been recorded on this system with different parameter settings than used here.

burst) component should bring the eye to exactly that position by the end of the burst. Mismatch of the burst and tonic components leads to either forward or backward drift following an undershoot or overshoot of the final eye position, known as postsaccadic drift. Studies in both humans and monkeys show that in the case of muscle weakening or nerve damage, which produces systematic undershooting of saccades, postsaccadic drift can be compensated for by adaptive processes that have time constants on the order of 1.5 days (Optican & Robinson, 1980). Ablation studies have shown that control of the burst and tonic gains is independent and that their control depends on different areas of the cerebellum. In addition, retinal slip has been shown to be a necessary and sufficient stimulus to elicit these adaptive changes (Optican & Miles, 1985).

To implement the memory structure for the burst gain in our burst generator, we have used a relatively new floating-gate structure that combines nonvolatile memory and computation into a single transistor. Floating-gate structures in VLSI (a metal oxide semiconductor transistor gate completely insulated from the circuitry by silicon dioxide) offer extremely effective analog parameter storage with retention measured in years. Until recently, however, the use of floating gates required the use of either ultraviolet (UV) radiation (Glasser, 1985; Mead, 1989a; Kerns, 1993) or bidirectional tunnel-

ing processes (Carley, 1989; Lande, Ranjbar, Ismail, & Berg, 1996) to modify the charge on the floating node, and both have significant drawbacks. The recent development of a complementary strategy of tunneling and hot electron injection (Hasler et al., 1995; Diorio, Mahajan, Hasler, Minch, & Mead, 1995) in a commercially available bipolar complementary metal oxide semiconductor process has alleviated some of these difficulties. Adding and removing electrons from the floating gate can be performed at extremely low rates, making it possible to create long training time constants.

To demonstrate the ability to reduce postsaccadic drift in our VLSI system, a sensitive direction-selective motion detector chip (Horiuchi & Koch, 1996) was mounted on the one-dimensional eye, and motion information was read from the chip 100 msec after the end of the saccadic burst activity. The burst activity period (lower trace in Figures 5A and 5B) is detected by reading a signal on the burst generator chip representing the suppression of the pause circuitry. A standard leftward saccade amplitude of about 23 degrees was programmed into the burst generator input, and a saccade was repeatedly triggered. The motion sensor was facing a stationary stripe stimulus, which would elicit a motion signal during and after the saccade burst.

The direction-of-motion information was summed across the motion detector array, and a simple, fixed-learning-rate algorithm was used to determine whether to increase or decrease the gain. One hundred msec after each trial saccade, the motion detector output current was compared against two threshold values. If the output value was greater than the rightward motion threshold, indicating overshoot, a unit hot-electron injection pulse was issued, which would reduce the floating-gate voltage and thus reduce the burst gain. If the integrated value was less than the leftward motion threshold, indicating undershoot, a unit tunneling pulse was issued, which would increase the floating-gate voltage and thus increase the pulse gain.

Figure 5A shows an experiment where the pulse gain was initialized to zero. With the particular learning rates used, eight trials were required before the gain was raised sufficiently to eliminate the postsaccadic drift. Figure 5B shows a similar experiment where the pulse gain was initialized to a large value. In this case, within 41 trials, the pulse gain was lowered sufficiently to eliminate the postsaccadic drift. The learning rates used in this example were arbitrary and can be set over many orders of magnitude.

2.5 Triggering the Saccade. Although the saccadic eye movements presented thus far were manually triggered for testing purposes, the system has also been extensively used with visual input to close the sensorimotor loop. In the initial stages of this project, visual input was provided to the saccadic system in the form of a simplified analog VLSI model of the retinocollicular visual pathway. This enabled the system to trigger orienting saccades to temporally changing visual stimuli (Horiuchi, Bishofberger, & Koch, 1994). This visually driven chip computed the centroid of temporal

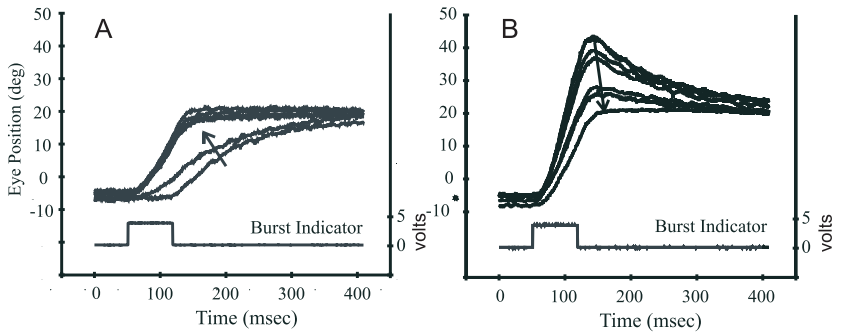

Figure 5: (A) Reduction of saccadic undershoot via on-chip learning. Saccade trajectories demonstrating the reduction of a backward postsaccadic drift by increasing the burst gain via a tunneling process that modifies the charge stored on a nonvolatile floating-gate memory circuit in an unsupervised manner. The circuit converged within eight practice saccades (not all shown). (B) Reduction of saccadic overshoot. Saccade trajectories showing the reduction of an onward postsaccadic drift by decreasing the burst gain via a hot-electron injection process, which modifies the charge on the same memory circuit as above but in the opposite direction. In this case, the performance converged in 41 practice saccades. The lower digital trace in each figure indicates the time of burst unit activity. The arrow indicates the progression from early saccade trials to later saccade trials. The floating-gate technology demonstrated here (Hasler et al., 1995; Diorio et al., 1995) provides us with a versatile, single transistor adaptive synapse.

activity in one dimension and triggered saccades when the sum of all the temporal-derivative signals on the array exceeded a threshold.

In other work, we have also triggered saccades to auditory targets using an analog VLSI model of auditory localization based on the barn owl auditory localization system (Horiuchi, 1995). Auditory saccades are interesting because sounds are most easily localized in the head-based coordinate frame, but eye movements (at the level of the saccadic burst generator) are specified in essentially retinotopic coordinates. A coordinate transform that compensates for different starting eye positions must be performed to specify saccades correctly to auditory targets.

3 Smooth Pursuit Eye Movements

While the saccadic system provides the primate with an effective alerting and orienting system to place targets in the fovea, in many cases, smooth

tracking of objects may be desirable to retain the high visual acuity of the fovea. The ability to move the eyes smoothly to stabilize wide-field visual motion is fairly universal, but the ability to select only a portion of the visual field to stabilize is highly developed only in primates. To accomplish this task, some mechanism is needed to define where the object is and from what part of the scene to extract motion information.

3.1 Visual Attention and Eye Movements. A number of studies have revealed the involvement of selective visual attention in the generation of both saccadic (Kowler, Anderson, Dosher, & Blaser, 1995; Hoffman & Subramaniam, 1995; Rafal, Calabresi, Brennan, & Scioltio, 1989; Shimojo, Tanaka, Hikosaka, & Miyauchi, 1995) and smooth pursuit eye movements (Khurana & Kowler, 1987; Ferrera & Lisberger, 1995; Tam & Ono, 1994). Attentional enhancement occurs at the target location just before a saccade, as well as at the target location during smooth pursuit. In the case of saccades, attempts to dissociate attention from the target location disrupt their accuracy and latency (Hoffman & Subramaniam, 1995). It has been proposed that attention is involved in programming the next saccade by highlighting the target location. For smooth pursuit—driven by visual motion in a negative feedback loop (Rashbass, 1961)—spatial attention is thought to be involved in the extraction of the target's motion. Since the cortical, motion-sensitive, middle temporal area (MT) and the middle superior temporal area (MST) have been strongly implicated in supplying visual motion information for pursuit by anatomical, lesion, and velocity-tuning studies, (see Lisberger, Morris, & Tychsen, 1987, for review) a mechanism to use the activity selectively from the neurons associated with the target at the correct time and place is actively being sought. The modulation of neural activity in these areas, for conditions that differ only by their instructions, has been investigated. Although only small differences in activity have been found in areas MT and MST during the initiation of smooth pursuit toward a target in the presence of a distractor (Ferrera & Lisberger, 1997), strong modulation of activity in MT and MST has been observed during an attentional task to discriminate between target and distractor motions (Treue & Maunsell, 1996).

Koch and Ullman (1985) proposed a model of attentional selection based on the output of a single saliency map by combining the activity of elementary feature maps in a topographic manner. The most salient locations are where activity from many different feature maps coincides, or at locations where activity from a preferentially weighted feature map, such as temporal change, occurs. A winner-take-all (WTA) mechanism, acting as the center of the attentional spotlight, selects the location with the highest saliency. While the WTA mechanism captures the idea of attending a single point target, many experiments have demonstrated weighted vector averaging in both saccadic and smooth pursuit behavior (Lisberger & Ferrera, 1997; Groh, Born, & Newsome, 1997; Watamaniuk & Heinen, 1994). Ana-

log circuits that can account for this diversity of responses (that is, vector averaging, winner-take-all, vector summation) need to be investigated.

3.2 An Attentional Tracking Chip. A number of VLSI-based visual tracking sensors that use a WTA attentional model have been described (Morris & DeWeerth, 1996; Brajovic & Kanade, 1998). Building on the work of Morris and DeWeerth (1996) on modeling selective visual attention, this chip incorporates focal-plane processing to compute image saliency and select a target feature for tracking. The target position and the direction of motion are reported as the target moves across the array, providing control signals for tracking eye movements.

The computational goal of the attentional tracking chip is the selection of a single target and the extraction of its retinal position and direction of motion. Figure 6 shows a block diagram of this computation. The first few upper stages of processing compute the saliency map from simple feature maps that drive the WTA-based selection of a target to track. Adaptive photoreceptor circuits (Delbrück, 1993) (at the top of Figure 6) transduce the incoming pattern of light into an array of voltages. The temporal (TD) and spatial (SD) derivatives are computed from these voltages and used to generate the saliency map and direction of motion. The saliency map is formed by summing the absolute value of each derivative (|TD| + |SD|). The direction-of-motion (DM) circuit computes a normalized product of the two derivatives:

$$\frac{TD \cdot SD}{|TD| + |SD|}.$$

Figure 7 shows an example stimulus and the computed features.

Only circuits at the WTA-selected location send information off-chip. These signals include the retinal position, the direction of motion, and the type of target being tracked. The saccadic system uses the position information to foveate the target, and the smooth pursuit system uses the motion information to match the speed of the target. The target's retinal position is reported by the position-to-voltage (P2V) circuit (DeWeerth, 1992) by driving the common position output line to a voltage representing its position in the array. The direction of motion is reported by a steering circuit that puts the local DM circuit's current onto the common motion-output line. The saccadic triggering (ST) circuit indicates whether the position of the target warrants a recentering saccade based on the distance of the target from the center of the array. This acceptance "window" is externally specified.

Figure 8 shows the response of the chip to a swinging edge stimulus. The direction of motion of the target (DM, upper trace) and the position of the target (P2V, lower trace) are displayed. As the target moves across the array, different direction-of-motion circuit outputs are switched onto the common output line. This switching is the primary cause of the noise seen on the motion output trace. At the end of the trace, the target slipped off

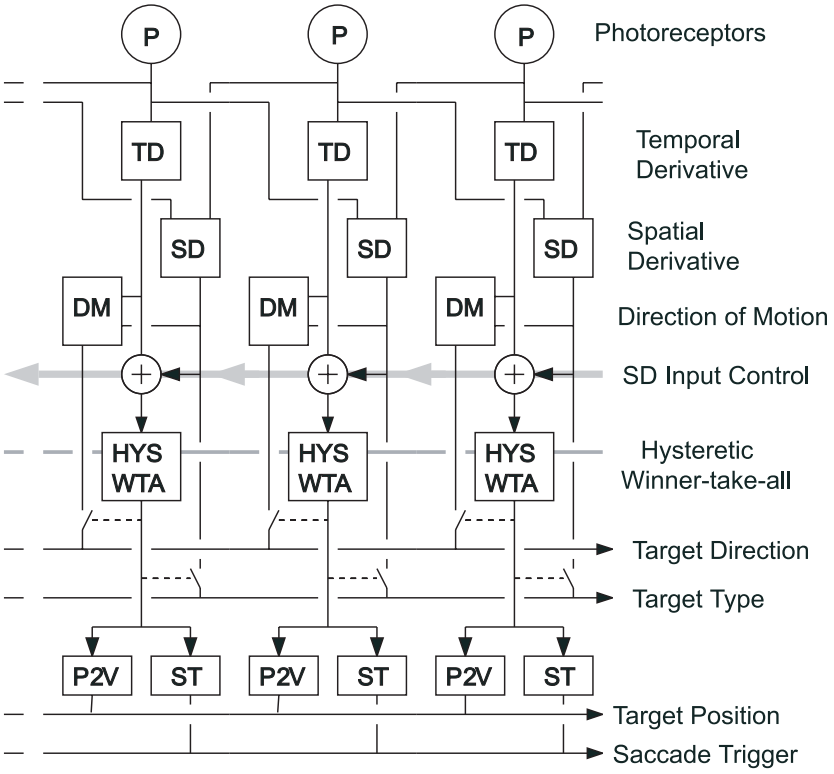

Figure 6: Block diagram of the visual tracking chip. Images are projected directly onto the chip surface's through a lens, and the output signals are sent to the oculomotor plant described in section 2. P = adaptive photoreceptor circuit, TD = temporal derivative circuit, SD = spatial derivative, DM = direction of motion, HYS WTA = hysteretic winner-take-all, P2V = position to voltage, ST = saccade trigger. The TD and SD signals are summed to form the saliency map from which the HYS WTA finds the maximum. Hysteresis is used locally to improve the tracking of moving targets, as well as to combat noise. The output of the HYS WTA steers both the direction of motion and the SD information onto global output lines. The HYS WTA also drives the P2V and ST circuits to convert the winning position to a voltage and to indicate when the selected pixel is outside a specified window located at the center of the array. The SD input control modulates the relative gain of the positive and negative spatial derivatives used in the saliency map. See the text for details.

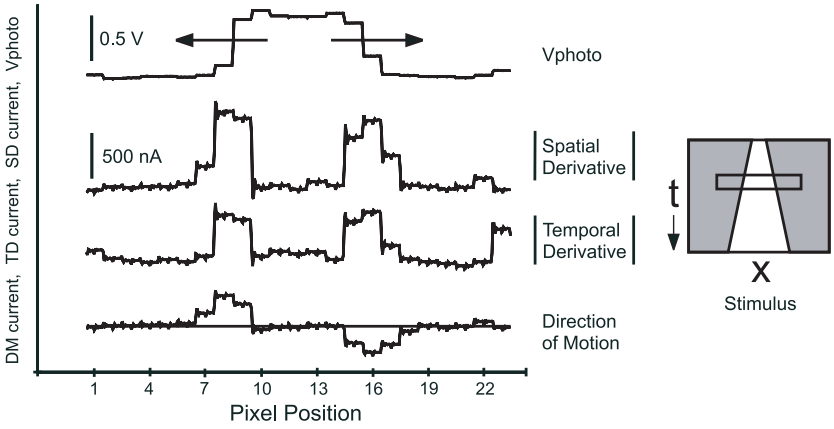

Figure 7: Example stimulus. Traces from top to bottom: Photoreceptor voltage, absolute value of the spatial derivative, absolute value of the temporal derivative, and direction of motion. The stimulus is a high-contrast, expanding bar (shown on the right), which provides two edges moving in opposite directions. The signed, temporal, and spatial derivative signals are used to compute the direction of motion shown in the bottom trace. The three lower traces were current measurements, which shows some clocking noise from the scanners used to obtain the data.

the photoreceptor array, and the winning status shifted to a location with a small background signal.

3.3 Visually Guided Tracking Eye Movements. To demonstrate smooth pursuit behavior in our one-dimensional system, we mounted the attentional tracking chip on the oculomotor system and used its visual processing outputs to drive both smooth pursuit and saccadic eye movements.

The motor component of the model used to drive smooth pursuit is based on a leaky integrator model described by McKenzie and Lisberger (1986) using only the target velocity input. Because retinal motion of the target serves as an eye-velocity error, direction-of-motion signals from the tracking chip are used as an eye acceleration command. Visual motion is thus temporally integrated to an eye velocity command and drives the oculomotor plant in parallel with the saccadic burst generator (see Figure 2).

To implement the smooth pursuit integrator in this system, off-chip circuits were constructed. The direction-of-motion signal from the tracking chip was split into leftward and rightward motion channels and used as eye acceleration commands, which were integrated to eye velocity com-

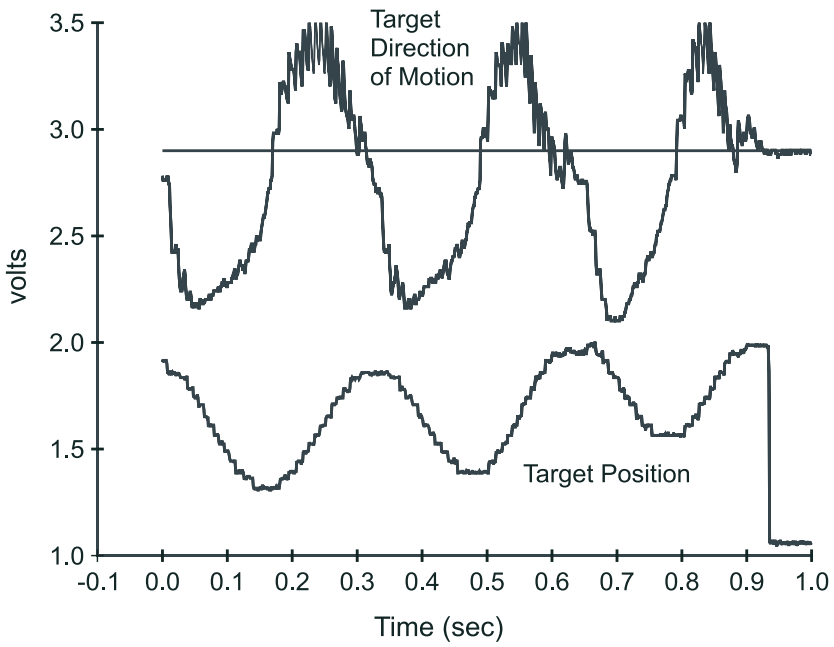

Figure 8: Extracting the target's position and direction of motion from a swinging target. The WTA output voltage is used to switch the DM current onto a common current-sensing line. The output of this signal, converted to a voltage, is seen in the top trace. The zero-motion level is indicated by the flat line shown at 2.9 volts. The lower trace shows the target's position from the position-to-voltage encoding circuits. The target's position and direction of motion are used to drive saccades and smooth pursuit eye movement during tracking. The noise in the upper trace is due to switching transients as WTA circuits switch in the DM currents from different pixel locations.

mands by the pursuit integrators (see Figure 2). The integrator leak time constants were set to about 1 sec.

Oscillation in the pursuit velocity around the target velocity (at around 6 Hz) is a common occurrence in primates (upper trace, Figure 10B) and is also seen in our system (but at about 4 Hz). Oscillations in this negative feedback system can occur from delays in visual processing and from large gain in the smooth pursuit integration stage. Our system has very little motion processing delay, but the gain on the integrator is large. Goldreich, Krauzlis, & Lisberger (1992) have shown that in the primate system, visual motion delays appear to be the dominant cause of this oscillation.

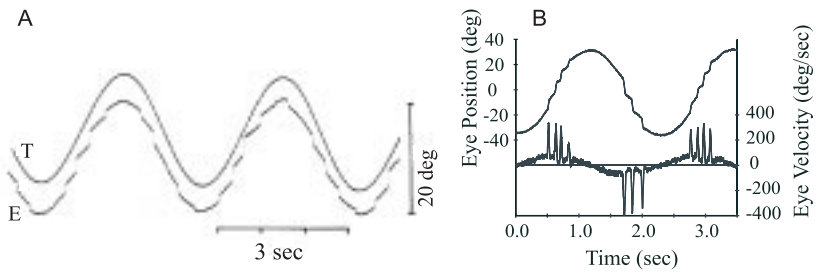

Figure 9: (A) Smooth pursuit and saccadic eye movements of a monkey in response to sinusoidal target motion at approximately 0.27 Hz, peak-to-peak amplitude 20 degrees. The target and eye position traces have been offset for clarity. (From Collewijn & Tamminga, 1984) (B) Smooth pursuit and saccadic eye movements in our VLSI model. A swinging target consisting of a bar with no distractors is tracked over a few cycles. The top trace shows the eye position over time, and the bottom trace shows the eye velocity.

When humans view natural scenes mixed with both stationary and moving objects, saccades and smooth pursuit are combined in an attempt to take in a scene quickly and scrutinize moving objects. How these two eye movements are behaviorally combined is still unclear. When humans or monkeys pursue fast, sinusoidally moving targets, the smooth pursuit eye movement becomes punctuated with catch-up saccades as the target speed exceeds the maximum pursuit speed and a retinal error builds up.

While visual motion provides the largest contribution to eye acceleration during the initiation and maintenance of pursuit, the target's retinal position and acceleration also contribute to driving the eye (Morris & Lisberger, 1985). In our hardware model, however, the pursuit system is driven by only the retinal velocity error. The saccadic system, dedicated to keeping targets near the center of the imager, uses position error to trigger and guide saccades. While these two motor control systems operate essentially independently, the visual target motion induced by the saccade must be suppressed at the input of the smooth pursuit integrator to prevent conflict between the two systems and to maintain the smooth pursuit eye velocity across saccades.

Figure 9B exemplifies the integration of saccadic with smooth pursuit eye movements during the tracking of a sinusoidally swinging target. When the velocity of the target exceeds the peak velocity of the pursuit system, the target slips out of the central region of the chip's field of view, and saccades are triggered to recenter the target.

In another experiment, we used a step-ramp stimulus to illustrate the separation of the saccadic and smooth pursuit systems, activating both systems

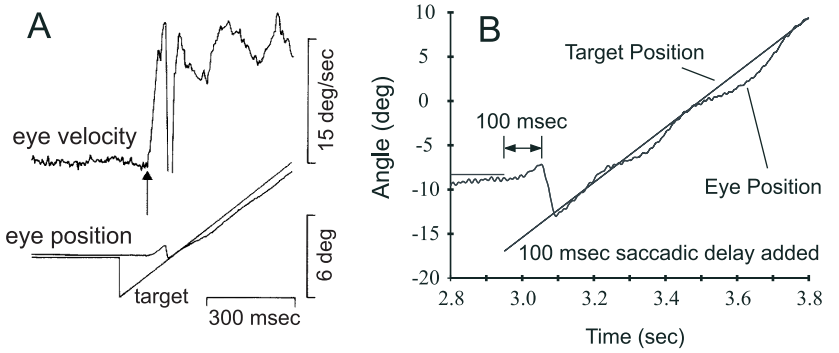

Figure 10: (A) Step-ramp experiment with a Macaque monkey. The upward arrow indicates the initialization of pursuit, which precedes the first saccade. (From Lisberger et al., 1987; with permission from *Annual Review of Neuroscience, 10*, ©1987, by Annual Reviews.) (B) Step-ramp experiment using the model. The target jumps from the fixation point to a new location and begins moving with constant velocity. An artificial delay of 100 msec has been added to simulate the saccadic triggering latency. Only the saccadic trigger is delayed; the target information is current.

at once but in different directions. In primates, visually triggered saccades (not including express saccades) have latencies from 150 to 250 msec; the pursuit system has a shorter latency, from 80 to 130 msec. With this stimulus, the pursuit system begins to move the eye in the direction of target motion before the saccade occurs (Lisberger et al., 1987). Because there is no explicit delay in the current saccadic triggering system, an artificial 100 msec delay was added in the saccadic trigger to mimic this behavior (see Figure 10A). The latency of the model pursuit system without adding additional delays is approximately 50 to 60 msec. Figure 10B shows comparison data from a step-ramp experiment in a macaque monkey.

4 Conclusions

The two-chip primate oculomotor system model presented in this article is part of an ongoing exploration into the issues of systems-level neurobiological modeling using neuromorphic analog VLSI. This work focuses on feedback systems that involve sensory and motor interaction with natural environments. Within the analog VLSI framework, it has touched on various examples of sensorimotor control, learning, and the coordination of different eye movements. Saccadic and smooth pursuit eye movements have been integrated in the system, which has raised many questions about

how to model their interaction. Adaptation of saccadic parameters based on biologically constrained error measures has been demonstrated. The use of a simple WTA model of visual attention for target selection and selective motion extraction has been demonstrated, raising many questions about the interaction between reflexive (collicular) and volitional (cortical) eye movement systems. Our ongoing work seeks to address many of these questions.

The main contribution of our work has been the demonstration of a real-time modeling system that brings together many different neural models to solve real-world tasks. To date, there are no other oculomotor modeling systems that use realistic burst generator circuits to drive an analog oculomotor plant with similar dynamics to the biological system. While other research groups have built biologically inspired, visual tracking systems, the problems they encounter are generally not similar to the problems faced by biological systems because they do not solve the task with hardware that has similar properties. By building circuits that compute with the representations of information found in the brain, the modeling system presented here is capable of replicating many of the behavioral, lesion, stimulation, and adaptation experiments performed on the primate oculomotor system. Armed with a continuously growing arsenal of circuits, we will be emulating much larger and more realistic sensorimotor systems in the future.

Acknowledgments

We thank Brooks Bishofberger for mechanical design of the oculomotor system and fabrication of some of the dynamics simulation electronics, Tobi Delbrück for advice on photoreceptor circuit layout, Paul Hasler for advice on the floating-gate structures, and Tonia Morris and Steven P. DeWeerth for their assistance and guidance in some important parts of the attentional selection circuits. We also thank Steven Lisberger, Rodney Douglas, and Terry Sejnowski for advice rendered over many years. The research reported here was supported by the Office of Naval Research and the Center for Neuromorphic Systems Engineering as part of the National Science Foundation Engineering Research Center Program.

References

Becker, W. (1989). Metrics. In R. H. Wurtz & M. E. Goldberg (Eds.), *The neurobiology of saccadic eye movements* (pp. 13–67). Amsterdam: Elsevier.

Boahen, K. (1997). The retinomorphic approach: Pixel-parallel adaptive amplification, filtering and quantization. *Analog Integ. Circ. Sig. Proc., 13*, 53–68.

Brajaovic, V., & Kanade, T. (1998). Computational sensor for visual tracking with attention. *IEEE J. of Solid-State Circuits, 33:8*, 1199–1207.

Carley, L. R. (1989). Trimming analog circuits using floating-gate analog MOS memory. *IEEE J. Solid State Circ., 24*, 1569–1575.

Collewijn, H., & Tamminga, E. P. (1984). Human smooth and saccadic eye movements during voluntary pursuit of different target motions on different back-

grounds. *J. Physiol., 351*, 217–250.
Collins, C. C., O'Meara, D., & Scott, A. B. (1975). Muscle tension during unrestrained human eye movements. *J. Physiol., 245*, 351–369.
Delbrück, T. (1993). Investigations of analog VLSI visual transduction and motion processing. Ph.D. Thesis, Computation and Neural Systems program, California Institute of Technology.
DeWeerth, S. P. (1992). Analog VLSI circuits for stimulus localization and centroid computation. *Intl. J. Comp. Vis., 8*, 191–202.
Diorio, C., Hasler, P., Minch, B., & Mead, C. (1997). A complementary pair of four-terminal silicon synapses. *Analog Integ. Circ. Sig. Proc., 13*, 153–166.
Diorio, C., Mahajan, S., Hasler, P., Minch, B., & Mead, C. (1995). A high-resolution non-volatile analog memory cell. In *Proc. of the Intl. Symp. on Circuits and Systems* (pp. 2233–2236). Seattle, WA.
Douglas, R., Mahowald, M., & Mead, C. (1995). Neuromorphic analogue VLSI. In W. M. Cowan, E. M. Shooter, C. F. Stevens, & R. F. Thompson (Eds.), *Annual reviews in neuroscience* (Vol. 18, pp. 255–281). Palo Alto, CA: Annual Reviews.
Elias, J. G. (1993). Artificial dendritic trees. *Neural Computation, 5*, 648–664.
Ferrera, V., & Lisberger, S. (1995). Attention and target selection for smooth pursuit eye movements. *J. Neurosci., 15*, 7472–7484.
Ferrera, V., & Lisberger, S. (1997). The effect of a moving distractor on the initiation of smooth-pursuit eye movements. *Visual Neuroscience, 14*, 323–338.
Fukushima, K., Yamaguchi, Y., Yasuda, M., & Nagata, S. (1970). An electronic model of the retina. *Proc. of the IEEE, 58*, 1950–1951.
Glasser, L. A. (1985). A UV write-enabled PROM. In H. Fuchs (Ed.), *Chapel Hill Conference on VLSI (1985)* (pp. 61–65). Rockville, MD: Computer Science Press.
Godaux, E., & Cheron, G. (1996). The hypothesis of the uniqueness of the oculomotor neural integrator—Direct experimental evidence in the cat. *J. Physiology London, 492*, 517–527.
Goldreich, D., Krauzlis, R. J., & Lisberger, S. G. (1992). Effect of changing feedback delay on spontaneous oscillations in smooth pursuit eye movements of monkeys. *J. Neurophysiol., 67*, 625–638.
Groh, J. M., Born, R. T., & Newsome, W. T. (1997). How is a sensory map read out? Effects of microstimulation in visual area MT on saccades and smooth pursuit eye movements. *J. Neurosci., 17*, 4312–4330.
Hasler, P., Diorio, C., Minch, B. A., & Mead, C. (1995). Single transistor learning synapses. In G. Tesauro, D. Touretzky, & T. Leen (Eds.), *Advances in neural information processing systems, 7* (pp. 817–824). Cambridge, MA: MIT Press.
Hepp, K., Henn, V., Vilis, T., & Cohen, B. (1989). Brainstem regions related to saccade generation. In R. H. Wurtz & M. E. Goldberg (Eds.), *The neurobiology of saccadic eye movements* (pp. 105–212). Amsterdam: Elsevier.
Hoffman, J., & Subramaniam, B. (1995). The role of visual attention in saccadic eye movements. *Perception and Psychophysics, 57*, 787–795.
Horiuchi, T. (1995). An auditory localization and coordinate transform chip. In G. Tesauro, D. Touretzky, & T. Leen (Eds.), *Advances in neural information processing systems 7* (pp. 787–794). Cambridge, MA: MIT Press.
Horiuchi, T., Bishofberger, B., & Koch, C. (1994). An analog VLSI saccadic system. In J. D. Cowan, G. Tesauro, and J. Alspector (Eds.), *Advances in neural information processing systems, 6* (pp. 582–589). San Mateo, CA: Morgan Kaufmann.

Horiuchi, T. K., & Koch, C. (1996). Analog VLSI circuits for visual motion-based adaptation of post-saccadic drift. In *Proc. 5th Intl. Conf. on Microelectronics for Neural Networks and Fuzzy Systems—MicroNeuro96* (pp. 60–66). Los Alamitos, CA: IEEE Computer Society Press.

Jürgens, R., Becker, W., & Kornhuber, H. H. (1981). Natural and drug-induced variations of velocity and duration of human saccadic eye movements: Evidence for a control of the neural pulse generator by local feedback. *Biol. Cybern., 39,* 87–96.

Kalayjian, Z., & Andreou, A. (1997). Asynchronous communication of 2D motion information using winner-take-all arbitration. *Analog Integ. Circ. Sig. Proc., 13,* 103–109.

Keller, E. L. (1973). Accommodative vergence in the alert monkey: Motor unit analysis. *Vision Res., 13,* 1565–1575.

Kerns, D. A. (1993). *Experiments in very large-scale analog computation*. Unpublished doctoral dissertation, California Institute of Technology.

Khurana, B., & Kowler, E. (1987). Shared attentional control of smooth eye movement and perception. *Vision Research, 27,* 1603–1618.

King, W. M., Lisberger, S. G., & Fuchs, A. F. (1986). Oblique saccadic eye movements. *J. Neurophysiol., 56,* 769–784.

Koch, C. (1989). Seeing chips: Analog VLSI circuits for computer vision. *Neural Computation, 1,* 184–200.

Koch, C., & Ullman, S. (1985). Shifts in selective visual attention: Towards the underlying neural circuitry. *Human Neurobiology, 4,* 219–227.

Kowler, E., Anderson, E., Dosher, B., & Blaser, E. (1995). The role of attention in the programming of saccades. *Vision Research, 35,* 1897–1916.

Lande, T. S., Ranjbar, H., Ismail, M., & Berg, Y. (1996). An analog floating-gate memory in a standard digital technology. In *Proc. 5th Intl. Conf. on Microelectronics for Neural Networks and Fuzzy Systems—MicroNeuro96* (pp. 271–276). Los Alamitos, CA: IEEE Computer Society Press.

Laughlin, S., van Steveninck, R. R. d., & Anderson, J. C. (1998). The metabolic cost of neural information. *Nature Neurosci., 1,* 36–41.

Lisberger, S. G., & Ferrera, V. P. (1997). Vector averaging for smooth pursuit eye movements initiated by two moving targets in monkeys. *J. Neurosci, 17,* 7490–7502.

Lisberger, S. G., Morris, E. J., & Tychsen, L. (1987). Visual motion processing and sensory-motor integration for smooth pursuit eye movements. In W. M. Cowan, E. M. Shooter, C. F. Stevens, & R. F. Thompson (Eds.), *Annual reviews in neuroscience, vol. 10* (pp. 97–129). Palo Alto, CA: Annual Reviews.

Mahowald, M. A. (1992). VLSI analogs of neuronal visual processing: A synthesis of form and function. Ph.D. Dissertation. Computer Science, California Insitute of Technology.

McKenzie, A., & Lisberger, S. G. (1986). Properties of signals that determine the amplitude and direction of saccadic eye movements in monkeys. *J. Neurophysiol., 56,* 196–207.

Mead, C. (1989a). Adaptive retina. In C. Mead & M. Ismail (Eds.), *Analog VLSI implementation of neural systems* (pp. 239–246). Boston: Kluwer.

Mead, C. (1989b). *Analog VLSI and neural systems.* Menlo Park, CA: Addison-Wesley.

Mead, C. (1990). Neuromorphic electronic systems. *Proc. IEEE, 78*, 1629–1636.

Morris, E. J., & Lisberger, S. G. (1985). A computer model that predicts monkey smooth pursuit eye movements on a millisecond timescale. *Soc. Neurosci. Abstr., 11*, 79.

Morris, T. G., & DeWeerth, S. P. (1996). Analog VLSI circuits for covert attentional shifts. In *Proc. 5th Intl. Conf. on Microelectronics for Neural Networks and Fuzzy Systems—MicroNeuro96* (pp. 30–37). Los Alamitos, CA: IEEE Computer Society Press.

Mortara, A. (1997). A pulsed communication / computation framework for analog VLSI perceptive systems. *Analog Integ. Circ. Sig. Proc., 13*, 93–101.

Nichols, M. J., & Sparks, D. L. (1995). Non-stationary properties of the saccadic system—New constraints on models of saccadic control. *J. Neurophysiol., 73*(1), 431–435.

Niebur, E., & Erdös, P. (1993). Theory of the locomotion of nematodes: Control of the somatic motor neurons by interneurons. *Mathematical Biosciences, 118*, 51–82.

Optican, L. M., & Miles, F. A. (1985). Visually induced adaptive changes in primate saccadic oculomotor control signals. *J. Neurophysiol., 54*, 940–958.

Optican, L. M., & Robinson, D. A. (1980). Cerebellar-dependent adaptive control of the primate saccadic system. *J. Neurophysiol., 44*, 1058–1076.

Rafal, R., Calabresi, P., Brennan, C., & Scioltio, T. (1989). Saccade preparation inhibits reorienting to recently attended locations. *J. Exp. Psych: Hum. Percep. Perf., 15*, 673–685.

Rashbass, C. (1961). The relationship between saccadic and smooth tracking eye movements. *J. Physiol., 159*, 326–338.

Robinson, D. (1973). Models of the saccadic eye movement control system. *Kybernetik, 14*, 71–83.

Sarpeshkar, R. (1997). *Efficient precise computation with noisy components: Extrapolating from electronics to neurobiology*. Unpublished manuscript.

Shimojo, S., Tanaka, Y., Hikosaka, O., & Miyauchi, S. (1995). Vision, attention, and action—Inhibition and facilitation in sensory motor links revealed by the reaction time and the line-motion. In T. Inui & J. L. McClelland (Eds.), *Attention and performance XVI*. Cambridge, MA: MIT Press.

Strassman, A., Highstein, S. M., & McCrea, R. A. (1986). Anatomy and physiology of saccadic burst neurons in the alert squirrel monkey. I. Excitatory burst neurons. *J. Comp. Neur., 249*, 337–357.

Tam, W. J., & Ono, H. (1994). Fixation disengagement and eye-movement latency. *Perception and Psychophysics, 56*, 251–260.

Treue, S., & Maunsell, J. (1996). Attentional modulation of visual motion processing in cortical areas MT and MST. *Nature, 382*, 539–541.

Watamaniuk, S. N. J., & Heinen, S. J. (1994). Smooth pursuit eye movements to dynamic random-dot stimuli. *Soc. Neuroscience Abstr., 20*, 317.

Westheimer, G. (1954). Mechanism of saccadic eye movements. *Arch. Ophthamol., 52*, 710.

Westheimer, G. A., & McKee, S. (1975). Visual acuity in the presence of retinal image motion. *J. Opt. Soc. Am, 65*, 847–850.

Received December 1, 1997; accepted June 15, 1998.